If the rate of deep-water formation is relatively low, however, or the hydrological cycle is fairly strong, the export of fresh water via NADW is reduced and the fresh water added in high latitudes tends to accumulate. There seems to be a critical threshold of freshwater input for maintaining the Atlantic thermohaline circulation. If the freshwater input is close to the threshold, the overturning becomes unstable and may oscillate over time. If the freshwater input exceeds the threshold, the haline effect overwhelms the thermal effect and the thermohaline circulation stops dead.

Manabe and Stouffer have projected that a four-fold increase in atmospheric $CO_2$ would increase the hydrological cycle sufficiently that the Atlantic thermohaline circulation might collapse. This would lead to a substantially deeper thermocline and a shift in the heat exchange between the hemispheres. It would also lead to a drastic reduction in the rate at which nutrients are supplied to the upper ocean biota and a reduction in the oxygen content of deep water.

## See also

**Antarctic Circumpolar Current. Conservative Elements. Ekman Transport and Pumping. Florida Current, Gulf Stream and Labrador Current. General Circulation Models. Heat Transport and Climate. North Sea Circulation.**

## Further Reading


Broecker WS (1991) The Great Ocean Conveyor. *Oceanography* 4: 79–89.

Cox M (1989) An idealized model of the world ocean. Part 1: The global scale water masses. *Journal of Physical Oceanography* 19: 1730–1752.

Gnanadesikan A (1999) A simple predictive model for the structure of the oceanic pycnocline. *Science* 283: 2077–2079.

Ledwell JR, Watson AJ and Law CS (1993) Evidence for slow mixing across the pycnocline from an open-ocean tracer-release experiment. *Nature* 364: 701–703.

McCartney MS and Talley LD (1984) Warm-to-cold water conversion in the northern North Atlantic Ocean. *Journal of Physical Oceanography* 14: 922–935.

Manabe S and Stouffer R (1993) Century-scale effects of increased atmospheric $CO_2$ on the ocean-atmosphere system. *Nature* 364: 215–218.

Rahmstorf S (1995) Bifurcations of the Atlantic thermohaline circulation in response to changes in the hydrological cycle. *Nature* 378: 145–149.

Rudels B, Jones EP, Anderson LG and Kattner G (1994) On the intermediate depth waters of the Arctic Ocean. In: *The Polar Oceans and their Role in Shaping the Global Environment*, *Geophysical Monograph 85*, pp. 33–46. Washington, DC: American Geophysical Union.

Schmitz WJ (1995) On the interbasin-scale thermohaline circulation. *Reviews of Geophysics* 33: 151–173.

Schmitz WJ and McCartney MS (1993) On the North Atlantic Circulation. *Reviews of Geophysics* 31: 29–49.

Schmitz WJ and Richardson PL (1991) On the sources of the Florida Current. *Deep-Sea Research* 38 (supplement 1): S379–S409.

Toggweiler JR and Samuels B (1995) Effect of Drake Passage on the global thermohaline circulation. *Deep-sea Research* 42: 477–500.

Toggweiler JR and Bjornsson H (2000) Drake Passage and paleoclimate. *Journal of Quaternary Science* 15: 319–328.

Toggweiler JR and Samuels B (1998) On the ocean's large-scale circulation near the limit of no vertical mixing. *Journal of Physical Oceanography* 28: 1832–1852.

Tziperman E (2000) Proximity of the present-day thermohaline circulation to an instability threshold. *Journal of Physical Oceanography* 30: 90–104.

Warren BA (1981) Deep circulation of the World Ocean. In: Warren BA and Wunsch C (eds) *Evolution of Physical Oceanography – Scientific Surveys in Honor of Henry Stommel*, pp. 6–41. Cambridge, MA: MIT Press.


# TERNS

*See* **LARIDAE, STERNIDAE AND RYNCHOPIDAE.**

# THREE-DIMENSIONAL (3D) TURBULENCE

**W. D. Smyth and J. N. Moum**,
Oregon State University, Corvallis, OR, USA



doi:10.1006/rwos.2001.0134

## Introduction

This article describes fluid turbulence with application to the Earth's oceans. We begin with the simple, classical picture of stationary, homogeneous,

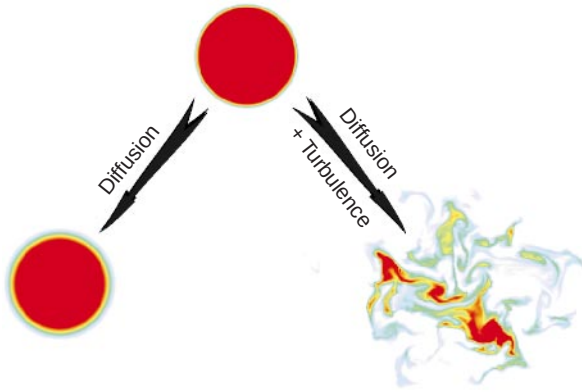


**Figure 1** A comparison of mixing enhanced by turbulence with mixing due to molecular processes alone, as revealed by a numerical solution of the equations of motion. The initial state includes a circular region of dyed fluid in a white background. Two possible evolutions are shown: one in which the fluid is motionless (save for random molecular motions), and one in which the fluid is in a state of fully developed, two-dimensional turbulence. The mixed region (yellow–blue) expands much more rapidly in the turbulent case.

isotropic turbulence. We then discuss departures from this idealized state that occur in small-scale geophysical flows. The discussion closes with a tour of some of the many physical regimes in which ocean turbulence has been observed.

Turbulent flow has been a source of fascination for centuries. The term 'turbulence' appears to have been used first in reference to fluid flows by da Vinci, who studied the phenomenon extensively. Today, turbulence is frequently characterized as the last great unsolved problem of classical physics. It plays a central role in both engineering and geophysical fluid flows. Its study led to the discovery of the first strange attractor by Lorenz in 1963, and thus to the modern science of chaotic dynamics. In the past few decades, tremendous insight into the physics of turbulence has been gained through theoretical and laboratory study, geophysical observations, improved experimental techniques, and computer simulations.

Turbulence results from the nonlinear nature of advection, which enables interaction between motions on different spatial scales. Consequently, an initial disturbance with a given characteristic length scale tends to spread to progressively larger and smaller scales. This expansion of the spectral range is limited at large scales by boundaries and/or body forces, and at small scales by viscosity. If the range of scales becomes sufficiently large, the flow takes a highly complex form whose details defy prediction.

The roles played by turbulence in the atmosphere and oceans can be classified into two categories: momentum transport and scalar mixing. In transporting momentum, turbulent motions behave in a manner roughly analogous to molecular viscosity, reducing differences in velocity between different regions of a flow. For example, winds transfer momentum to the Earth via strong turbulence in the planetary boundary layer (a kilometer-thick layer adjacent to the ground) and are thus decelerated.

Scalar mixing refers to the homogenization of fluid properties such as temperature by random molecular motions. Molecular mixing rates are proportional to spatial gradients, which are greatly amplified due to the stretching and kneading (i.e. stirring) of fluid parcels by turbulence. This process is illustrated in **Figure 1**, which shows the evolution of an initially circular region of dyed fluid in a numerical simulation. Under the action of molecular mixing (or diffusion) alone, an annular region of intermediate shade gradually expands as the dyed fluid mixes with the surrounding fluid. If the flow is turbulent, the result is dramatically different. The circle is distended into a highly complex shape, and the region of mixed fluid expands rapidly.

## The Mechanics of Turbulence

**Figure 2** illustrates the main physical mechanisms that drive turbulence at the smallest scales. The description is presented in terms of strain and vorticity, quantities that represent the tendency of the flow at any point to deform and to rotate fluid parcels, respectively. A major and recent insight is that vorticity and strain are not distributed

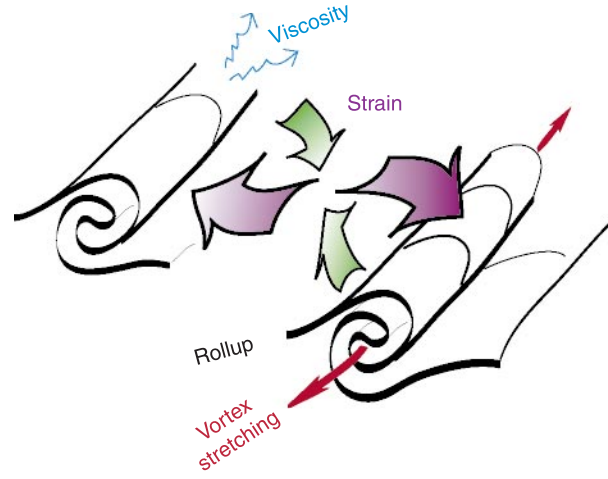


**Figure 2** Schematic illustration of line vortices and strained regions in turbulent flow. Fluid parcels in the vortex interiors rotate with only weak deformation. In contrast, fluid parcels moving between the vortices are rapidly elongated in the direction of the purple arrows and compressed in the direction of the green arrows.

randomly in turbulent flow, but rather are concentrated into coherent regions, each of which is dominated by one type of motion or the other. The first mechanism we consider is vortex rollup due to shear instability. This process results in a vorticity concentration of dimension close to unity, i.e. a line vortex. Line vortices are reinforced by the process of vortex stretching. When a vortex is stretched by the surrounding flow, its rotation rate increases to conserve angular momentum. Opposing these processes is molecular viscosity, which both dissipates vorticity and fluxes it away from strongly rotational regions.

Turbulence may thus be visualized as a loosely tangled 'spaghetti' of line vortices, which continuously advect each other in complex ways (**Figure 3**). At any given time, some vortices are being created via rollup, some are growing due to vortex stretching, and some are decaying due to viscosity. Many, however, are in a state of approximate equilibrium among these processes, so that they appear as long-lived, coherent features of the flow. Mixing is not accomplished within the vortices themselves; in fact, these regions are relatively stable, like the eye of a hurricane. Instead, mixing occurs mainly in regions of intense strain that exist between any two nearby vortices that rotate in the same sense (**Figure 2**). It is in these regions that fluid parcels are deformed to produce amplified gradients and consequent rapid mixing.

## Stationary, Homogeneous, Isotropic Turbulence

Although the essential structures of turbulence are not complex (**Figure 2**), they combine in a bewildering range of sizes and orientations that defies analysis (**Figure 3**). Because of this, turbulence is most usefully understood in statistical terms. Although the statistical approach precludes detailed prediction of flow evolution, it does give access to the rates of mixing and property transport, which are of primary importance in most applications. Statistical analyses focus on the various moments of the flow field, defined with respect to some averaging operation. The average may be taken over space and/or time, or it may be an ensemble average taken over many flows begun with similar initial conditions.

Analyses are often simplified using three standard assumptions. The flow statistics are assumed to be

- stationary (invariant with respect to translations in time),
- homogeneous (invariant with respect to translations in space), and/or
- isotropic (invariant with respect to rotations).

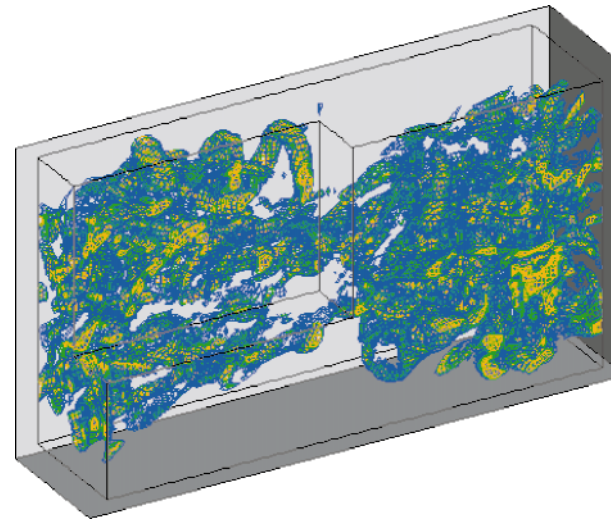

**Figure 3** Computer simulation of turbulence as it is believed to occur in the ocean thermocline. The colored meshes indicate surfaces of constant vorticity.

Much of our present understanding pertains to this highly idealized case. Our description will focus on the power spectra that describe spatial variability of kinetic energy and scalar variance. The spectra provide insight into the physical processes that govern motion and mixing at different spatial scales.

### Velocity Fields

> Big whorls have little whorls
> That feed on their velocity
> And little whorls have lesser whorls
> And so on to viscosity
> L.F. Richardson (1922)

Suppose that turbulence is generated by a steady, homogeneous, isotropic stirring force whose spatial variability is described by the Fourier wavenumber $k_F$. Suppose further that the turbulence is allowed to evolve until equilibrium is reached between forcing and viscous dissipation, i.e., the turbulence is statistically stationary.

**Figure 4** shows typical wavenumber spectra of kinetic energy, $E(k)$, and kinetic energy dissipation, $D(k)$, for such a flow. $E(k)\mathrm{d}k$ is the kinetic energy contained in motions whose wavenumber magnitudes lie in an interval of width $\mathrm{d}k$ surrounding $k$. $D(k)\mathrm{d}k = \nu k^2 E(k)\mathrm{d}k$ is the rate at which that kinetic energy is dissipated by molecular viscosity ($\nu$) in that wavenumber band. The net rate of energy dissipation is given by $\varepsilon = \int_0^\infty D(k)\mathrm{d}k$, and is equal (in the equilibrium state) to the rate at which energy is supplied by the stirring force.

Nonlinear interactions induce a spectral flux, or cascade, of energy. The energy cascade is directed

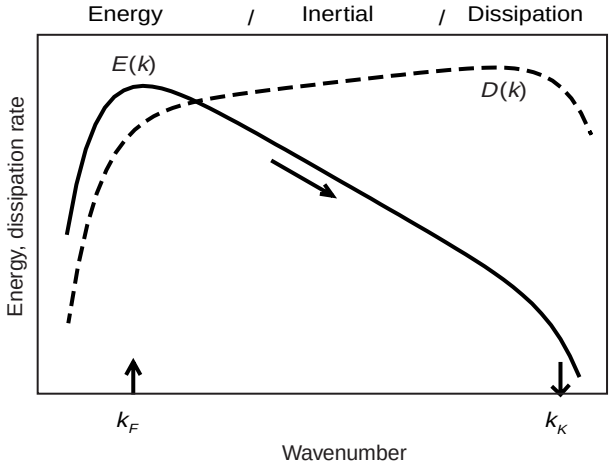


**Figure 4** Theoretical wavenumber spectra of kinetic energy and kinetic energy dissipation for stationary, homogeneous, isotropic turbulence forced at wavenumber $k_F$. Approximate locations of the energy containing, inertial, and dissipation subranges are indicated, along with the Kolmogorov wavenumber $k_K$. Axes are logarithmic. Numerical values depend on $R_e$ and are omitted here for clarity.

primarily (though not entirely) toward smaller scales, i.e., large-scale motions interact to create smaller-scale motions. The resulting small eddies involve sharp velocity gradients, and are therefore susceptible to viscous dissipation. Thus, although kinetic energy resides mostly in large-scale motions, it is dissipated primarily by small-scale motions. (Note that the logarithmic axes used in **Figure 4** tend to de-emphasize the peaks in the energy and dissipation rate spectra.) Turbulence can be envisioned as a 'pipeline' conducting kinetic energy through wavenumber space: in at the large scales, down the spectrum, and out again at the small scales, all at a rate $\varepsilon$. The cascade concept was first suggested early in the twentieth century by L.F. Richardson, who immortalized his idea in the verse quoted at the beginning of this section.

The energy spectrum is often divided conceptually into three sections. The energy-containing subrange encompasses the largest scales of motion, whereas the dissipation subrange includes the smallest scales. If the range of scales is large enough, there may exist an intermediate range in which the form of the spectrum is independent of both large-scale forcing and small-scale viscous effects. This intermediate range is called the inertial subrange. The existence of the inertial subrange depends on the value of the Reynolds number: $R_e = u\ell/\nu$, where $u$ and $\ell$ are scales of velocity and length characterizing the energy-containing range. The spectral distance between the energy-containing subrange and the dissipation subrange, $k_F/k_K$, is proportional to $R_e^{3/4}$. A true inertial subrange exists only in the limit of large $R_e$.

In the 1940 s, the Russian statistician A.N. Kolmogorov hypothesized that, in the limit $R_e \to \infty$, the distribution of eddy sizes in the inertial and dissipation ranges should depend on only two parameters (besides wavenumber): the dissipation rate $\varepsilon$ and the viscosity $\nu$, i.e., $E = E(k; \varepsilon, \nu)$. Dimensional reasoning then implies that $E = \varepsilon^{1/4}\nu^{5/4} f(k/k_K)$, where $k_K = (\varepsilon/\nu^3)^{1/4}$ is the Kolmogorov wavenumber and $f$ is some universal function. Thus, with the assumptions of stationarity, homogeneity, isotropy, and infinite Reynolds number, all types of turbulence, from flow over a wing to convection in the interior of the sun, appear as manifestations of a single process whose form depends only on the viscosity of the fluid and the rate at which energy is transferred through the 'pipeline'. This tremendous simplification is generally regarded as the beginning of the modern era of turbulence theory.

Kolmogorov went on to suggest that the spectrum in the inertial range should be simpler still by virtue of being independent of viscosity. In that case $E = E(k, \varepsilon)$, and the function can be predicted from dimensional reasoning alone up to the universal constant $C_K$, namely, $E = C_K \varepsilon^{2/3} k^{-5/3}$. This power-law spectral form indicates that motions in the inertial subrange are self-similar, i.e., their geometry is invariant under coordinate dilations.

Early efforts to identify the inertial subrange in laboratory flows were inconclusive because the Reynolds number could not be made large enough. (In a typical, laboratory-scale water channel, $u \sim 0.1\,\mathrm{m\,s^{-1}}$, $\ell \sim 0.1\,\mathrm{m}$, and $\nu \sim 10^{-6}\,\mathrm{m^2\,s^{-1}}$, giving $R_e \sim 10^4$. In a typical wind tunnel, $u \sim 1\,\mathrm{m\,s^{-1}}$, $\ell \sim 1\,\mathrm{m}$, and $\nu \sim 10^{-5}\,\mathrm{m^2\,s^{-1}}$, so that $R_e \sim 10^5$.) The inertial subrange spectrum was first verified in 1962 using measurements in a strongly turbulent tidal channel near Vancouver Island, where typical turbulent velocity scales $u \sim 1\,\mathrm{m\,s^{-1}}$ and length scales $\ell \sim 100\,\mathrm{m}$ combine with the kinematic viscosity of seawater $\nu \sim 10^{-6}\,\mathrm{m^2\,s^{-1}}$ to produce a Reynolds number $R_e \sim 10^8$. From this experiment and others like it, the value of $C_K$ has been determined to be near 1.6.

### Passive Scalars and Mixing

Now let us suppose that the fluid possesses some scalar property $\theta$, such as temperature or the concentration of some chemical species, and that the scalar is dynamically passive, i.e., its presence does not affect the flow. (In the case of temperature, this is true only for sufficiently small-scale fluctuations; see Buoyancy Effects later in this article for details.) Suppose also that there is a source of large-scale

variations in $\theta$, e.g., an ambient temperature gradient in the ocean. Isosurfaces of $\theta$ will be folded and kneaded by the turbulence so that their surface area tends to increase. As a result, typical gradients of $\theta$ will also increase, and will become susceptible to erosion by molecular diffusion. Scalar variance is destroyed at a rate $\chi$, which is equal (in equilibrium) to the rate at which variance is produced by the large eddies.

Thus, the turbulent mixing of the scalar proceeds in a manner similar to the energy cascade discussed above. However, there is an important difference in the two phenomena. Unlike energy, scalar variance is driven to small scales by a combination of two processes. First, scalar gradients are compressed by the strain fields between the turbulent eddies. Second, the eddies themselves are continually redistributed toward smaller scales. (The latter process is just the energy cascade described in the previous section.)

**Figure 5** shows the equilibrium scalar variance spectrum for the case of heat mixing in water. Most of the variance is contained in the large scales, which are separated from the small scales by an inertial-convective subrange (so-called because temperature variance is convected by motions in the inertial subrange of the energy spectrum). Here, the spectrum depends only on $\varepsilon$ and $\chi$; its form is $E_\theta = \beta\chi\varepsilon^{-1/3}k^{-5/3}$, where $\beta$ is a universal constant.

The shape of the spectrum at small scales is very different from that of the energy spectrum, owing to the fact that, in sea water, the molecular diffusivity, $\kappa$, of heat is smaller than the kinematic viscosity. The ratio of viscosity to thermal diffusivity is termed the Prandtl number (i.e. $P_r = \nu/\kappa$) and has a value near 7 for sea water. In the viscous-convective subrange, the downscale cascade of temperature variance is slowed because the eddies driving the cascade are weakened by viscosity. In other words, the first of the two processes listed above as driving the scalar variance cascade is no longer active. There is no corresponding weakening of temperature gradients, because molecular diffusivity is not active on these scales. As a result, there is a tendency for variance to 'accumulate' in this region of the spectrum and the spectral slope is reduced from $-5/3$ to $-1$. However, the variance in this range is ultimately driven into the viscous-diffusive subrange, where it is finally dissipated by molecular diffusion. A measure of the wavenumber at which scalar variance is dissipated is the Batchelor wavenumber, $k_B = (\varepsilon/\nu\kappa^2)^{1/4}$. When $P_r > 1$, as for sea water, the Batchelor wavenumber is larger than the Kolmogorov wavenumber, i.e., temperature fluctuations can exist at smaller scales than velocity fluctuations.

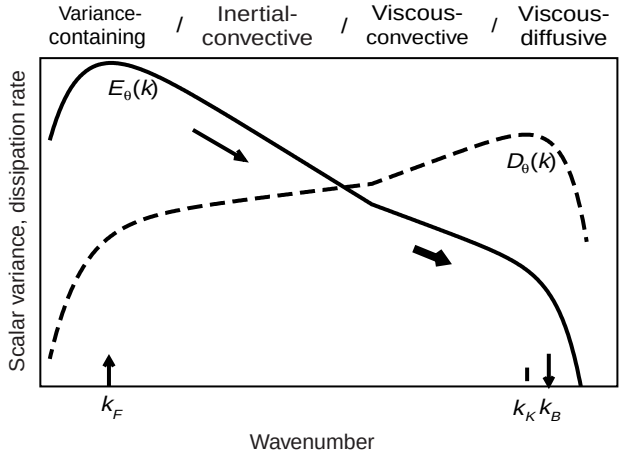


**Figure 5** Theoretical wavenumber spectra of scalar variance and dissipation for stationary, homogeneous, isotropic turbulence forced at wavenumber $k_F$. Approximate locations of the variance-containing, inertial-convective, viscous-convective, and viscous-diffusive subranges are indicated, along with the Kolmogorov wavenumber $k_K$ and the Batchelor wavenumber $k_B$. Axes are logarithmic. Numerical values depend on $R_e$ and are omitted here for clarity.

In summary, the energy and temperature spectra exhibit many similarities. Energy (temperature variance) is input at large scales, cascaded down the spectrum by inertial (convective) processes, and finally dissipated by molecular viscosity (diffusion). The main difference between the two spectra is the viscous-convective range of the temperature spectrum, in which molecular smoothing acts on the velocity field but not on the temperature field. This difference is even more pronounced if the scalar field represents salinity rather than temperature, for salinity is diffused even more weakly than heat. The ratio of the molecular diffusivities of heat and salt is of order $10^2$, so that the smallest scales of salinity fluctuation in sea water are ten times smaller than those of temperature fluctuations.

## Turbulence in Geophysical Flows

The assumptions of homogeneity, stationarity and isotropy as employed by Kolmogorov have permitted tremendous advances in our understanding of turbulence. In addition, approximations based on these assumptions are used routinely in all areas of turbulence research. However, we must ultimately confront the fact that physical flows rarely conform to our simplifying assumptions. In geophysical turbulence, symmetries are upset by a complex interplay of effects. Here, we focus on three important classes of phenomena that modify small-scale

turbulence in the ocean: shear, stratification, and boundary proximity.

### Shear Effects

Geophysical turbulence often occurs in the presence of a current which varies on scales much larger than the energy-containing scales of the turbulence, and evolves much more slowly than the turbulence. Examples include atmospheric jet streams and large-scale ocean currents such as the Gulf Stream and the Equatorial Undercurrent. In such cases, it makes sense to think of the background current as an entity separate from the turbulent component of the flow.

Shear upsets homogeneity and isotropy by deforming turbulent eddies. By virtue of the resulting anisotropy, turbulent eddies exchange energy with the background shear through the mechanism of Reynolds stresses. Reynolds stresses represent correlations between velocity components parallel to and perpendicular to the background flow, correlations that would vanish if the turbulence were isotropic. Physically, they represent transport of momentum by the turbulence. If the transport is directed counter to the shear, kinetic energy is transferred from the background flow to the turbulence. This energy transfer is one of the most common generation mechanisms for geophysical turbulence.

In sheared turbulence, the background shear acts primarily on the largest eddies. Motions on scales much smaller than the Corrsin scale, $L_C = \sqrt{\varepsilon/S^3}$ (where $S = \mathrm{d}U/\mathrm{d}z$, the vertical gradient of the ambient horizontal current) are largely unaffected.

### Buoyancy Effects

Most geophysical flows are affected to some degree by buoyancy forces, which arise due to spatial variations in density. Buoyancy breaks the symmetry of the flow by favoring the direction in which the gravitational force acts. Buoyancy effects can either force or damp turbulence. Forcing occurs in the case of unstable density stratification, i.e., when heavy fluid overlies light fluid. This happens in the atmosphere on warm days, when the air is heated from below. The resulting turbulence is often made visible by cumulus clouds. In the ocean, surface cooling (at night) has a similar effect. Unstable stratification in the ocean can also result from evaporation, which increases surface salinity and hence surface density. In each of these cases, unstable stratification results in convective turbulence, which can be extremely vigorous. Convective turbulence usually restores the fluid to a stable state soon after the destabilizing flux ceases (e.g., when the sun rises over the ocean).

Buoyancy effects tend to damp turbulence in the case of stable stratification, i.e., when light fluid overlies heavier fluid. In stable stratification, a fluid parcel displaced from equilibrium oscillates vertically with frequency $N = \sqrt{-g\rho^{-1}\mathrm{d}\rho/\mathrm{d}z}$, the buoyancy or Brunt–Vaisala frequency ($g$ represents acceleration due to gravity and $\rho(z)$ is the ambient mass density). A result of stable stratification that can dramatically alter the physics of turbulence is the presence of internal gravity waves (IGW). These are similar to the more familiar interfacial waves that occur at the surfaces of oceans and lakes, but continuous density variation adds the possibility of vertical propagation. Visible manifestations of IGW include banded clouds in the atmosphere and slicks on the ocean surface. IGW carry momentum, but no scalar flux and no vorticity.

In strongly stable stratification, motions may be visualized approximately as two-dimensional turbulence (**Figure 1**) flowing on nearly horizontal surfaces that undulate with the passage of IGW. The quasi-two-dimensional mode of motion carries all of the vorticity of the flow (since IGW carry none), and is therefore called the vortical mode.

In moderately stable stratification, three-dimensional turbulence is possible, but its structure is modified by the buoyancy force, particularly at large scales. Besides producing anisotropy, the suppression of vertical motion damps the transfer of energy from any background shear, thus reducing the intensity of turbulence. On scales much smaller than the Ozmidov scale, $L_0 = \sqrt{\varepsilon/N^3}$, buoyancy has only a minor effect. (In Passive scalars and mixing above, we used temperature as an example of a dynamically passive quantity. This approximation is valid only on scales smaller than the Ozmidov scale.) The relative importance of stratification and shear depends on the magnitudes of $S$ and $N$. If $S \gg N$, shear dominates and turbulence is amplified. On the other hand, if $S \ll N$, the buoyancy forces dominate and turbulence is suppressed.

The relationship between IGW and turbulence in stratified flow is exceedingly complex. At scales in excess of a few meters (**Figure 6**), ocean current fluctuations behave like IGW, displaying the characteristic spectral slope $k^{-1}$. At scales smaller than the Ozmidov scale (typically a few tens of centimeters), fluctuations differ little from the classical picture of homogeneous, isotropic turbulence. The intermediate regime is a murky mix of nonlinear IGW and anisotropic turbulence that is not well understood at present.

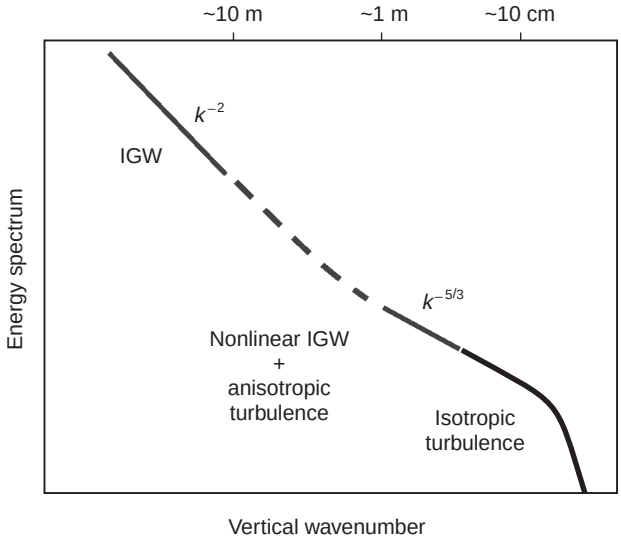


**Figure 6** Energy spectrum (cf. **Figure 4**) extended to larger scales to include internal gravity waves (IGW) plus anisotropic stratified turbulence. Labels represent approximate length scales from ocean observations.

The breaking of IGW is thought to be the major source of turbulence in the ocean interior. Breaking occurs when a superposition of IGW generates locally strong shear and/or weak stratification. IGW propagating obliquely in a background shear may break on encountering a critical level, a depth at which the background flow speed equals the horizontal component of the wave's phase velocity. (Many dramatic phenomena occur where wave speed matches flow speed; other examples include the hydraulic jump and the sonic boom.) Just as waves may generate turbulence, turbulent motions in stratified flow may radiate energy in the form of waves.

In stably stratified turbulence, the distinction between stirring and mixing of scalar properties becomes crucial. Stirring refers to the advection and deformation of fluid parcels by turbulent motion, whereas mixing involves actual changes in the scalar properties of fluid parcels. Mixing can only be accomplished by molecular diffusion, though it is accelerated greatly in turbulent flow due to stirring (cf. **Figure 1** and the accompanying discussion). In stable stratification, changes in the density field due to stirring are reversible, i.e., they can be undone by gravity. In contrast, mixing is irreversible, and thus leads to a permanent change in the properties of the fluid. For example, consider a blob of water that has been warmed at the ocean surface, then carried downward by turbulent motions. If the blob is mixed with the surrounding water, its heat will remain in the ocean interior, whereas if the blob is only stirred, it will eventually bob back up to the surface and return its heat to the atmosphere.

### Boundary Effects

It is becoming increasingly clear that most turbulent mixing in the ocean takes place near boundaries, either the solid boundary at the ocean bottom, or the moving boundary at the surface. All boundaries tend to suppress motions perpendicular to themselves, thus upsetting both the homogeneity and the isotropy of the turbulence. Solid boundaries also suppress motion in the tangential directions. Therefore, since the velocity must change from zero at the boundary to some nonzero value in the interior, a shear is set up, leading to the formation of a turbulent boundary layer. Turbulent boundary layers are analogous to viscous boundary layers, and are sites of intense, shear-driven mixing (**Figure 7**). In turbulent boundary layers, the characteristic size of the largest eddies is proportional to the distance from the boundary.

Near the ocean surface, the flexible nature of the boundaries leads to a multitude of interesting phenomena, notably surface gravity waves and Langmuir cells. These phenomena contribute significantly to upper-ocean mixing and thus to air–sea fluxes of momentum, heat and various chemical species. Boundaries also include obstacles to the flow, such as islands and seamounts, which create turbulence. If flow over an obstacle is stably stratified, buoyancy-accelerated bottom flow and a downstream hydraulic jump may drive turbulence (**Figure 7**).

Ocean turbulence is often influenced by combinations of shear, stratification, and boundary effects. In the example shown in **Figure 7**, all three effects combine to create an intensely turbulent flow that diverges dramatically from the classical picture of stationary, homogeneous, isotropic turbulence.

## Length Scales of Ocean Turbulence

Examples of turbulent flow regimes that have been observed in the ocean can be considered in terms of typical values of $\varepsilon$ and $N$ that pertain to each (**Figure 8**). This provides the information to estimate both largest and smallest scales present in the flow. The largest scale is approximated by the Ozmidov scale, which varies from a few centimeters in the ocean's thermocline to several hundred meters in weakly stratified and/or highly energetic flows. The smallest scale, the Kolmogorov scale $L_K = k_K^{-1}$, is typically 1 cm or less.

Turbulence in the upper ocean mixed layer may be driven by wind and/or by convection due to

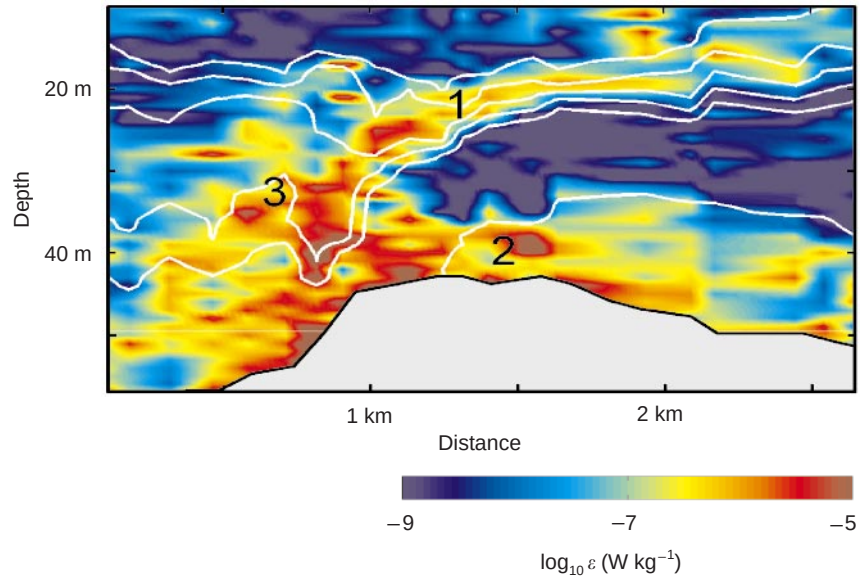


**Figure 7** Flow over Stonewall bank, on the continental shelf off the Oregon coast. Colors show the kinetic energy dissipation rate, with red indicating strong turbulence. White contours are isopycnals, showing the effect of density variations in driving the downslope flow. Three distinct turbulence regimes are visible: (1) turbulence driven by shear at the top of the rapidly moving lower layer, (2) a turbulent bottom boundary layer and (3) a hydraulic jump.

surface cooling. In the convectively mixed layer, $N$ is effectively zero within the turbulent region, and the maximum length scale is determined by the depth of the mixed layer. In both cases the free surface limits length scale growth.

Turbulence in the upper equatorial thermocline is enhanced by the presence of shear associated with the strong equatorial zonal current system. Stratification tends to be considerably stronger in the upper thermocline than in the main thermocline. Despite weak stratification, turbulence in the main thermocline tends to be relatively weak due to isolation from strong forcing. Turbulence in this region is generated primarily by IGW interactions.

Tidal channels are sites of extremely intense turbulence, forced by interactions between strong tidal currents and three-dimensional topography. Length scales are limited by the geometry of the channel. Turbulent length scales in the bottom boundary layer are limited below by the solid boundary and above by stratification. Intense turbulence is also found in hydraulically controlled flows, such as have been found in the Strait of Gibraltar, and also over topography on the continental shelf (cf. **Figure 7**). In these flows the stratification represents a potential energy supply that drives strongly sheared downslope currents, the kinetic energy of which is in turn converted into turbulence and mixing.

All of these turbulence regimes are subjects of ongoing observational and theoretical research, aimed at generalizing Kolmogorov's view of turbulence to encompass the complexity of real geophysical flows.

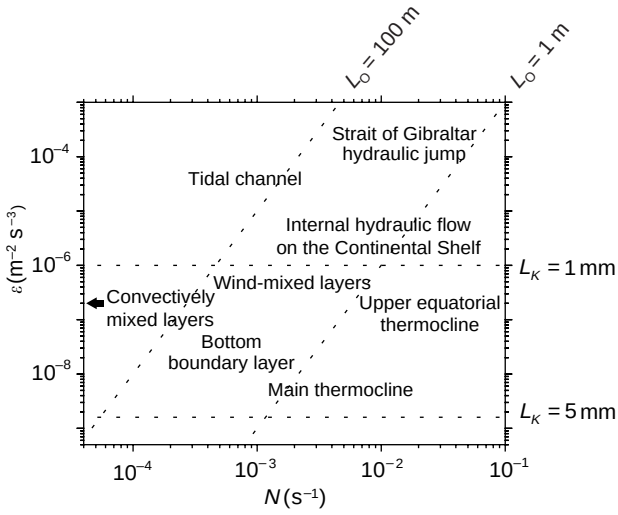


**Figure 8** Regimes of ocean turbulence located with respect to stratification and energy dissipation. Dotted lines indicate Ozmidov and Kolmogorov length scales.

## See also

**Atlantic Ocean Equatorial Currents. Brazil and Falklands (Malvinas) Currents. Breaking Waves**

**and Near-surface Turbulence. Heat and Momentum Fluxes at the Sea Surface. Heat Transport and Climate. Indian Ocean Equatorial Currents. Internal Waves. Island Wakes. Langmuir Circulation and Instability. Mesoscale Eddies. Open Ocean Convection. Pacific Ocean Equatorial Currents. Turbulence in the Benthic Boundary Layer. Upper Ocean Mixing Processes. Vortical Modes.**

## Further Reading

Frisch U (1995) *Turbulence*. Cambridge: Cambridge University Press.

Hunt JCR, Phillips OM and Williams D (1991) *Turbulence and Stochastic Processes; Kolmogoroff's Ideas 50 Years On*. London: The Royal Society.

Kundu PK (1990) *Fluid Mechanics*. London: Academic Press.

# TIDAL ENERGY

**A. M. Gorlov**, Northeastern University, Boston Massachusetts, USA



doi:10.1006/rwos.2001.0032

## Introduction

Gravitational forces between the moon, the sun and the earth cause the rhythmic rising and lowering of ocean waters around the world that results in Tide Waves. The moon exerts more than twice as great a force on the tides as the sun due to its much closer position to the earth. As a result, the tide closely follows the moon during its rotation around the earth, creating diurnal tide and ebb cycles at any particular ocean surface. The amplitude or height of the tide wave is very small in the open ocean where it measures several centimeters in the center of the wave distributed over hundreds of kilometers. However, the tide can increase dramatically when it reaches continental shelves, bringing huge masses of water into narrow bays and river estuaries along a coastline. For instance, the tides in the Bay of Fundy in Canada are the greatest in the world, with amplitude between 16 and 17 meters near shore. High tides close to these figures can be observed at many other sites worldwide, such as the Bristol Channel in England, the Kimberly coast of Australia, and the Okhotsk Sea of Russia. **Table 1** contains ranges of amplitude for some locations with large tides.

On most coasts tidal fluctuation consists of two floods and two ebbs, with a semidiurnal period of about 12 hours and 25 minutes. However, there are some coasts where tides are twice as long (diurnal tides) or are mixed, with a diurnal inequality, but are still diurnal or semidiurnal in period. The magnitude of tides changes during each lunar month. The highest tides, called spring tides, occur when the moon, earth and sun are positioned close to a straight line (moon syzygy). The lowest tides, called neap tides, occur when the earth, moon and sun are at right angles to each other (moon quadrature). Isaac Newton formulated the phenomenon first as follows: 'The ocean must flow twice and ebb twice, each day, and the highest water occurs at the third hour after the approach of the luminaries to the meridian of the place'. The first tide tables with accurate prediction of tidal amplitudes were published by the British Admiralty in 1833. However, information about tide fluctuations was available long before that time from a fourteenth century British atlas, for example.

Rising and receding tides along a shoreline area can be explained in the following way. A low height tide wave of hundreds of kilometers in diameter runs on the ocean surface under the moon, following its rotation around the earth, until the wave hits a continental shore. The water mass moved by the moon's gravitational pull fills narrow bays and river estuaries where it has no way to escape and spread over the ocean. This leads to interference of waves and accumulation of water inside these bays and estuaries, resulting in dramatic rises of the water level (tide cycle). The tide starts receding as the moon continues its travel further over the land, away from the ocean, reducing its gravitational influence on the ocean waters (ebb cycle).

**Table 1** Highest tides (tide ranges) of the global ocean

| *Country* | *Site* | *Tide range* (m) |
|---|---|---|
| Canada | Bay of Fundy | 16.2 |
| England | Severn Estuary | 14.5 |
| France | Port of Ganville | 14.7 |
| France | La Rance | 13.5 |
| Argentina | Puerto Rio Gallegos | 13.3 |
| Russia | Bay of Mezen (White Sea) | 10.0 |
| Russia | Penzhinskaya Guba (Sea of Okhotsk) | 13.4 |